

Maresin 1 Promotes Wound Healing and Socket Bone Regeneration for Alveolar Ridge Preservation

Journal of Dental Research
2020, Vol. 99(8) 930–937
© The Author(s) 2020



Article reuse guidelines:
sagepub.com/journals-permissions
DOI: 10.1177/0022034520917903
journals.sagepub.com/home/jdr

C.W. Wang¹ , S.H. Yu¹, T. Fretwurst², L. Larsson^{1,3}, J.V. Sugai^{1,4}, J. Oh¹, K. Lehner¹, Q. Jin⁵, and W.V. Giannobile^{1,4,6} 

Abstract

Tooth extraction results in alveolar bone resorption and is accompanied by postoperative swelling and pain. Maresin 1 (MaR1) is a proresolving lipid mediator produced by macrophages during the resolution phase of inflammation, bridging healing and tissue regeneration. The aim of this study was to examine the effects of MaR1 on tooth extraction socket wound healing in a preclinical rat model. The maxillary right first molars of Sprague-Dawley rats were extracted, and gelatin scaffolds were placed into the sockets with or without MaR1. Topical application was also given twice a week until complete socket wound closure up to 14 d. Immediate postoperative pain was assessed by 3 scores. Histology and microcomputed tomography were used to assess socket bone fill and alveolar ridge dimensional changes at selected dates. The assessments of coded specimens were performed by masked, calibrated examiners. Local application of MaR1 potentially accelerated extraction socket healing. Macroscopic and histologic analysis revealed a reduced soft tissue wound opening and more rapid re-epithelialization with MaR1 delivery versus vehicle on socket healing. Under micro-computed tomography analysis, MaR1 (especially at 0.05 µg/µL) stimulated greater socket bone fill at day 10 as compared with the vehicle-treated animals, resulting in less buccal plate resorption and a wider alveolar ridge by day 21. Interestingly, an increased ratio of CD206⁺:CD68⁺ macrophages was identified in the sockets with MaR1 application under immunohistochemistry and immunofluorescence analysis. As compared with the vehicle therapy, local delivery of MaR1 reduced immediate postoperative surrogate pain score panels. In summary, MaR1 accelerated extraction wound healing, promoted socket bone fill, preserved alveolar ridge bone, and reduced postoperative pain in vivo with a rodent preclinical model. Local administration of MaR1 offers clinical potential to accelerate extraction socket wound healing for more predictable dental implant reconstruction.

Keywords: tooth extraction, re-epithelialization, alveolar resorption, alveolar bone loss, macrophage, mediators of inflammation

Introduction

Dental extractions are one of the most common oral surgical procedures performed on humans. Tooth removal, especially surgical extractions, can lead to significant postoperative complications, including pain, swelling, infection, and mastication deficiency (Bui et al. 2003). In addition, alveolar ridge remodeling following the extraction can lead to resorption of nearly half of the alveolar bone width (Schropp et al. 2003; Araujo and Lindhe 2005; Avila-Ortiz et al. 2014), which may complicate tooth replacement with implant therapy. Therefore, alveolar ridge preservation procedures, such as placement of bone grafts, barrier membranes, and/or biological agents, have been developed to limit alveolar bone resorption following tooth removal (Pagni et al. 2012; Bassir et al. 2018). Alveolar ridge preservation procedures can only partially prevent the resorption of the ridge, and delayed healing may occur at the grafted site, with the quality of the regenerated bone being unpredictable. Therefore, there is a need to develop a local therapeutic agent to enhance the healing of an extraction wound to reduce postextraction complications and promote bone regeneration for future implant installation and functional restoration.

Maresin 1 (MaR1) is an endogenous anti-inflammatory and proresolving mediator produced mainly by macrophages (Serhan et al. 2009; Serhan et al. 2012). Macrophages have been shown to play a major role in resolving inflammation and

¹Department of Periodontics and Oral Medicine, School of Dentistry, University of Michigan, Ann Arbor, MI, USA

²Department of Oral and Craniomaxillofacial Surgery, Faculty of Medicine, Medical Center—University of Freiburg, Freiburg, Germany

³Department of Periodontology, Institute of Odontology, University of Gothenburg, Goteborg, Sweden

⁴Biointerfaces Institute, University of Michigan, Ann Arbor, MI, USA

⁵Department of Cariology, Restorative Sciences and Endodontics, University of Michigan, Ann Arbor, MI, USA

⁶Department of Biomedical Engineering, College of Engineering, University of Michigan, Ann Arbor, MI, USA

A supplemental appendix to this article is available online.

Corresponding Author:

C.W. Wang, Department of Periodontics and Oral Medicine, School of Dentistry, University of Michigan, 1011 North University Avenue, Ann Arbor, MI 48109-1078, USA.

Email: jeffwa@umich.edu

promoting wound healing and tissue regeneration (Das et al. 2015; Garlet and Giannobile 2018; Viniegra et al. 2018). It has also been shown that M2-like macrophages produce more MaR1 as compared with M1-like macrophages (Dalli and Serhan 2012). MaR1 is likely to be a key mediator at the interface between the resolution of inflammation and the phases of tissue healing and regeneration. Initially, MaR1 was isolated from self-limited inflammatory exudate, and its specialized bioactions, such as enhancing phagocytosis and efferocytosis, were demonstrated as signals for resolution of inflammation (Serhan et al. 2009; Serhan 2014). Later, its complete stereochemistry was established with total organic synthesis achieved, and its ability to promote tissue regeneration and control inflammatory pain was further proven (Serhan et al. 2012). Additionally, it was demonstrated that MaR1 facilitates healing of vascular injury (Akagi et al. 2015) and is organ protective in a lung inflammation model and a colitis model in mice (Marcon et al. 2013; Abdounour et al. 2014; Krishnamoorthy et al. 2015). Given that MaR1 exerts such potent proresolving and regenerative potential, it seems likely that MaR1 would enhance the oral wound healing required to facilitate extraction repair.

The aim of this study was to investigate the effects of topical MaR1 administration on extraction wound healing and alveolar bone remodeling in a rodent animal model.

Materials and Methods

Rat Tooth Extraction Model

The experimental protocol was approved by the Institutional Animal Care and Use Committee at the University of Michigan in accordance with the *Guide for the Care and Use of Laboratory Animals*. The Unit for Laboratory Animal Medicine facilitated all animal procurement and care at the University of Michigan. This study conformed with ARRIVE guidelines for preclinical studies. Sprague-Dawley rats (male, 3 to 5 wk of age, 2 to 3 rats/cage) were obtained from a commercial vendor (Charles River) and acclimated for at least 5 d before the experiments. A few animals with residual roots were excluded from the study and analysis. The total included number of rats were 71: 23 for vehicle control (12 for 10 d and 11 for 21 d), 18 each for 0.5 and 0.05 $\mu\text{g}/\mu\text{L}$ of MaR1 (8 for 10 d and 10 for 21 d), 8 for 0.01 $\mu\text{g}/\mu\text{L}$, and 4 for 0.001 $\mu\text{g}/\mu\text{L}$. Under general anesthesia via ketamine (50 mg/kg) and xylazine (10 mg/kg), maxillary right first molars were carefully extracted (C.W.W.) under magnification (3.5 \times) with luxators to avoid fracture of the roots following the established protocols (Lin et al. 2011). Gelatin sponges (Gelfoam; Pfizer Pharmaceutical) absorbed with either vehicle (5 μL of normal saline) or MaR1 (0.5, 0.05, 0.01, 0.001 $\mu\text{g}/\mu\text{L}$) were then placed into the extraction sockets depending on the randomized allocation of the animals. The total quantity of MaR1 that was applied to the wound was 2.5, 0.25, 0.05, and 0.005 μg per socket. The extraction sockets were then sealed with tissue glue (n-butyl cyanoacrylate, PeriAcryl [GluStitch Inc.]; Fig. 1A). The extraction wound was treated topically with saline (2 μL) in the vehicle group or MaR1 (2 μL per concentration) twice weekly until complete

closure of the extraction sites was observed. Control and experimental groups were always housed separately for the quality assurance of the treatment. The housing condition was the same among all groups, and no diet modifications were made in this study.

Micro-computed tomography Assessment

The animals were euthanized by CO₂ overdose at the designated time points (days 10 and 21). The maxillary segments were dissected and fixed in 10% neutral-buffered formalin for 2 d and then transferred to 70% alcohol before micro-computed tomography (microCT) scanning. The harvested specimens were scanned with a microCT scanning system (eXplore Locus, GE Healthcare; Scanco μCT -100, Medical AG) at 10- to 18- μm voxel resolution with an energy level of 70 to 80 kV (Kuroshima et al. 2013). The scans were reconstructed to produce 2- and 3-dimensional images of the maxillary specimens, and all microCT assessments were performed by masked examiner (S.H.Y.). The GEMS MicroView software was used for the analysis (Parallax Innovations Inc.). The extraction sockets of the mesial roots were isolated by manual contouring and analyzed with regard to the percentage of bone fill. The dimensional change of the alveolar ridge was evaluated with the frontal view of the alveolar ridge 1 mm mesial from the second molar over the extraction socket and with the cemento-enamel junction as a reference to calculate the vertical height loss at the buccal, middle, and lingual (V1 to V3) crestal surfaces. Alveolar ridge width was measured from the most crestal point of the alveolar ridge with 0.2-mm incremental descending levels to capture the morphology of the alveolar bone (H1 to H3).

Histologic, Immunohistochemical, and Immunofluorescence Analysis

Histologic analysis was performed following a previously established protocol (Jin et al. 2004). Following microCT scanning, the block specimens were decalcified for 14 d in 10% EDTA solution. The harvested maxillae were then embedded in paraffin, sectioned sagittally along the long axis of the extraction socket into sections of 4- to 5- μm thickness with a microtome, and stained with hematoxylin and eosin. Then images of sections were captured at 2 \times and 4 \times magnification with a Nikon Eclipse E800 microscope (Nikon) fitted with a SPOT-2 Camera (Diagnostic Instruments). Image Pro Plus software (Media Cybernetics) was used for further histologic analysis. The wound opening dimensions and epithelial thickness above the mesial root of the extraction socket were measured by masked examiner (T.F.).

Samples for immunohistochemistry were dewaxed and incubated overnight at 60 °C in DIVA antigen-retrieval solution (Biocare Medical). Following blocking of endogenous peroxidase, the sections were incubated with primary antibody for 60 min at room temperature. The sections were then incubated with the MACH4 horseradish peroxidase-labeled

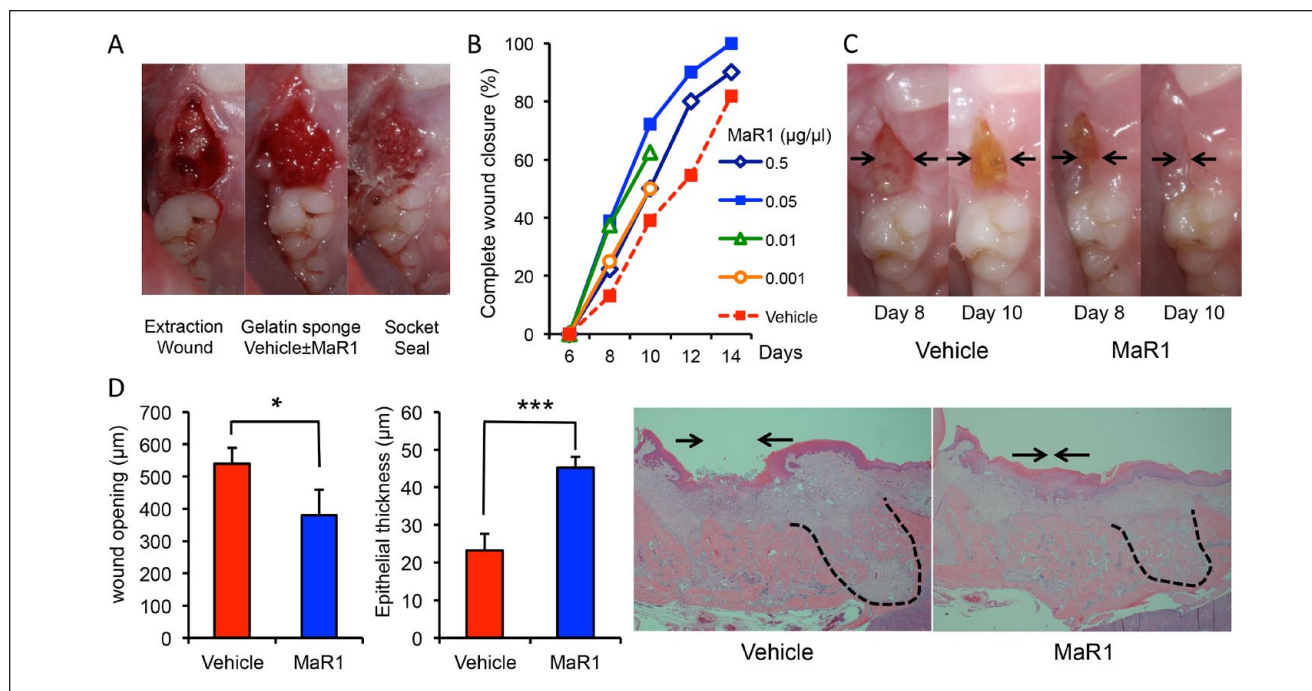


Figure 1. Maresin I (MaR1) accelerates wound closure following tooth extraction. **(A)** The maxillary right first molars of rats were extracted, and a gelatin sponge was placed into each socket with vehicle (5 μ L, saline) or MaR1 (0.5, 0.05, 0.01, and 0.001 μ g/ μ L). The socket was sealed with cyanoacrylate glue. **(B)** The extraction wound was treated and observed every 2 d. $n = 18$ to 23 per group ($n = 8$ for 0.01 and $n = 4$ for 0.001 μ g/ μ L of MaR1, observed up to 10 d only). **(C)** Representative preclinical images in the same animal at days 8 and 10. Arrows indicate the remaining extraction wound opening. **(D)** MaR1 facilitates extraction wound re-epithelialization. The animals were sacrificed, and the maxillae were processed and stained with hematoxylin and eosin for histologic analysis. The extraction wounds were assessed by a masked examiner under light microscopy (4 \times). Right insets are the representative sagittal sections of the extraction sockets. Note the remaining wound opening over the control socket (arrows). The mesial root socket is also outlined with black dotted lines. $n = 6$ per group. Results are presented as mean \pm SEM. * $P < 0.05$ and *** $P < 0.001$ vs. vehicle control.

polymer (Biocare Medical). Positive cells were detected with DAB substrate (Biocare Medical). Hematoxylin was used for counterstaining of the sections. The antibodies and dilutions used were CD206 (1:1500, No. 64693; Abcam) and CD68 (1:100, No. 31630; Abcam). Negative controls were performed by omitting the primary antibodies for both markers.

The other sections after antigen retrieval were incubated with 3% bovine serum albumin for blocking of nonspecific binding, followed by incubation overnight at 4 $^{\circ}$ C with the following primary antibodies: mouse anti-CD68 (ab31630; Abcam) diluted 1:50 or rabbit anti-CD206 (ab64693; Abcam) diluted 1:1,000. The sections were then incubated with Alexa-conjugated secondary antibodies for 2 h (Alexa 488 goat anti-mouse, diluted 1:200; Alexa 555 donkey anti-rabbit, diluted 1:200; Abcam), rinsed, and mounted with Prolong Mounting Medium (Invitrogen) containing DAPI to visualize DNA content. Omission of primary antibody was used as negative control. Fluorescence images were taken under 10 \times and 20 \times magnification (EVOS FL Auto 2; Invitrogen) and merged with EVOS Imaging Software. The sockets were divided into 3 components (coronal, middle, and apical), and the positive cells were counted in each section by a masked experienced investigator (L.L.).

Postoperative Pain Assessment

Three pain score assessments were utilized to monitor the pain levels of the rats, including a grimace scale (Sotocinal et al. 2011; Oliver et al. 2014), tube chewing, and burrowing time (modified from Wodarski et al. 2016). Standardized chewing tubes were placed in each cage and collected every 48 h to assess the level of tube destruction (C.W.W. and T.F.). The tube-chewing scale was as follows: 1 = minor biting defect, 2 = major biting defect but the circle integrity of the tube remained, 3 = the circle integrity was destroyed, and 4 = all pieces were <2 cm (i.e., score of 4 indicates less pain, with the tube mostly destroyed). For the grimace scale and modified burrowing time, rats were acclimated in each cage with the lid opened for 5 min; two 30-s video clips were then randomly taken and assessed by 2 independent, calibrated, and masked examiners (S.H.Y. and T.F.). Calibration sessions were performed by reviewing the videos by the 2 masked examiners prior to independent assessment. Interexaminer agreement was achieved with a kappa of 0.72 (95% CI, 0.54 to 0.90). Intraexaminer agreement showed a kappa of 0.76 (95% CI, 0.59 to 0.94) for S.H.Y. and 0.80 (95% CI, 0.64 to 0.96) for T.F. The scores of the 2 examiners were averaged for the final results.

Statistical Analysis

Statistical analyses were performed with analysis of variance and post hoc Student's *t* test comparing experimental and control groups. Multiple Bonferroni corrections were applied when multiple concentrations of MaR1 were evaluated. An α level of 0.05 was used for statistical significance if not otherwise specified. Results are presented as mean \pm SEM.

Results

MaR1 Accelerates Tooth Extraction Soft Tissue Wound Closure

After extraction of the first molars, topical application of MaR1 accelerated the complete closure of the extraction wound. All concentrations of MaR1 exhibited trends of acceleratory kinetics, and no animal exhibited any signs of an adverse event to the treatment. At 10 d, MaR1 at a concentration of 0.05 $\mu\text{g}/\mu\text{L}$ showed maximal efficacy, with >72% of animals reaching complete wound closure as compared with vehicles at around 39% (Fig. 1B). In general, MaR1 application shifted the healing approximately 2 to 4 d faster as compared with the controls. The clinical wound closure was confirmed from sagittal histologic sections showing that with MaR1 treatment (0.05 $\mu\text{g}/\mu\text{L}$), there was significantly less wound opening (379 vs. 539 μm : MaR1 vs. vehicle, $P < 0.05$) and a thicker epithelium above the mesial root socket (Fig. 1D).

MaR1 Promotes Socket Bone Fill and Preserves the Alveolar Ridge

MaR1 promoted socket bone fill with various concentrations, with the highest potency at 0.05 $\mu\text{g}/\mu\text{L}$ concentration, which showed an increase of 16% of bone fill at 10 d (Fig. 2A). The sockets were completely healed, with similar bone density of the alveolar bone in both groups after 21 d (data not shown). Additionally, the alveolar bone ridge in the sites treated with MaR1 application displayed less buccal bone resorption (Fig. 2B, C). MaR1 (at 0.5 and 0.05 $\mu\text{g}/\mu\text{L}$) resulted in a significantly wider crestal alveolar ridge dimension as compared with vehicle (1.30 vs. 1.23 vs. 0.87 mm: 0.5 $\mu\text{g}/\mu\text{L}$ vs. 0.05 $\mu\text{g}/\mu\text{L}$ vs. vehicle, $P < 0.01$) and less vertical buccal bone resorption (0.37 vs. 0.29 vs. 0.55 mm, $P < 0.05$). Basal bone width (H2 and H3) as well as vertical ridge resorption at the midcrest (V2) and lingual side (V3) did not show significant differences among the groups.

MaR1 Regulates the Relative Expression of M2-like Macrophage Surface Marker CD206

Here we investigated if MaR1 could enhance the expression of M2-like macrophage surface marker CD206. We found that 10nM MaR1 could reduce M1 marker HLA-DR and upregulate CD206 expression (Appendix Fig. 2). Additionally, MaR1

at 0.05 $\mu\text{g}/\mu\text{L}$ increased the CD206- to CD68-positive macrophage ratio in the extraction socket after 10 d of healing. Of note, MaR1 did not affect CD68⁺ but did slightly increase CD206⁺ cell number. When the CD206⁺:CD68⁺ ratio was considered, there was a significant increase with MaR1 application (0.98 vs. 0.72: MaR1 vs. control, $P < 0.05$; Fig. 3A) as well as the relative ratio of double-positive cells (Fig. 3B).

MaR1 Reduces Postoperative Pain Scores

The combined concentrations of the MaR1 group showed a significant reduction of immediate postoperative pain, particularly at 1 d after tooth extraction (Fig. 4). With MaR1 application, the animals exhibited significantly lower grimace scale scores (2.8 vs. 4.8: MaR1 vs. vehicle, $P < 0.01$; Fig. 4A). The tube-chewing scores were also significantly higher (the higher destructions to the tubes, the less pain) in the MaR1 group as compared with the vehicle group (3.1 vs. 2.2, $P < 0.01$) at 1 d; however, the difference between the 2 groups was insignificant at 3 d, and both groups returned to their preoperative pain levels (Fig. 4B). Modified burrowing time also showed that the MaR1 rats tended to spend less time in the tube as compared with the vehicle group (54 vs. 91 s, $P < 0.05$; Fig. 4C).

Discussion

In this study, we investigated the therapeutic potential of MaR1 on tooth extraction wound healing, including soft and hard tissue repair in rats. The results showed that topical application of MaR1 reduced immediate postoperative pain scores, accelerated soft tissue wound closure, stimulated faster socket bone fill, and better preserved the alveolar bone ridge. The application of MaR1 increased the relative number of M2-like macrophages in the healing socket. Taken together, the results indicate that MaR1 aids in tooth extraction wound healing, thereby enabling favorable dental implant rehabilitation.

MaR1 accelerated extraction wound healing, resulting in a mean 2- to 4-d faster rate in complete wound closure. When the wound repair time course is compared between humans and rodents, rats metabolize and heal much more rapidly (Amler et al. 1960; Aguirre et al. 2010; Lin et al. 2011; Vieira et al. 2015). Therefore, molar extraction socket healing in rats took about only 2 wk for soft tissue wound closure. As compared with humans, this period may be 6 wk or even longer. In terms of the potential mechanism to facilitate extraction wound closure, in a similar context (skin wound healing in an animal model) MaR1 was shown to reduce skin edema and decrease levels of proinflammatory cytokines and reactive oxygen species (i.e., myeloperoxidase; Cezar et al. 2019). Furthermore, MaR1 may not be directly regulating the epithelial cells but promoting the resolution of the inflammation that drives the acceleration of the wound closure. Our findings demonstrated that TNF- α can inhibit keratinocyte proliferation (Appendix Fig. 1). MaR1 has been demonstrated to inhibit the production of TNF- α from macrophages (Gong et al. 2014). These

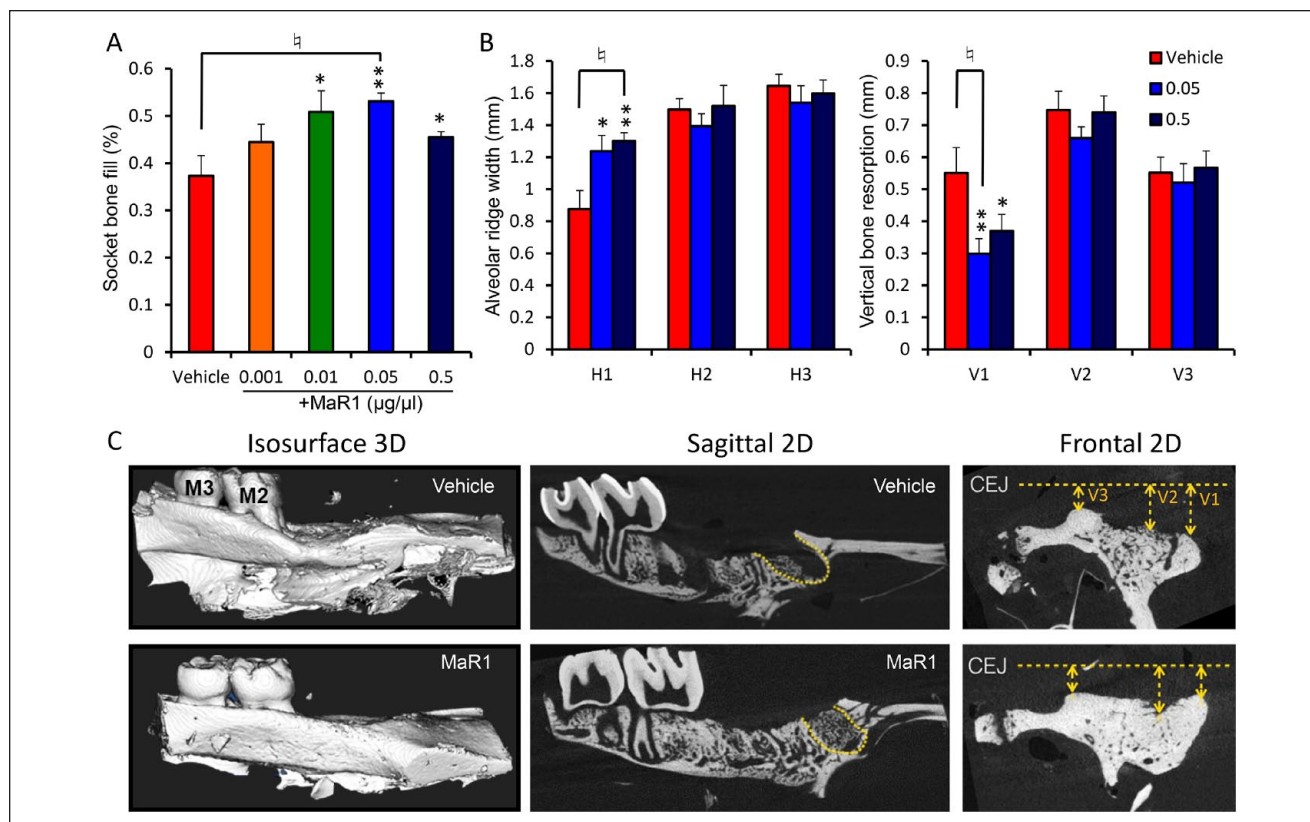


Figure 2. Maresin 1 (MaR1) stimulates extraction socket bone fill and preserves the alveolar ridge. **(A)** Micro-computed tomography (microCT) analysis by a masked examiner of socket bone fill after 10 d of healing. $n = 8$ to 12 per group ($n = 4$ for 0.001 $\mu\text{g}/\mu\text{L}$ of MaR1). **(B)** MicroCT assessment of the frontal view of the alveolar ridge dimension and resorption after 21 d of healing. V1 is the vertical resorption from the cemento-enamel junction (CEJ) of the buccal plate; V2 is the middle; and V3 is the lingual crest. H1 to H3 represent the alveolar ridge width with 0.2-mm incremental descending levels from the peak of the crest. Results are presented as mean \pm SEM. * $P < 0.05$ and ** $P < 0.01$ vs. vehicle. $^{\#}P < 0.05$ after Bonferroni correction vs. vehicle. **(C)** Representative microCT images of the alveolar bone ridge in each group are shown. The mesial root socket, where socket bone fill measurements were performed, is outlined with yellow dotted lines.

findings may demonstrate an indirect mechanism of MaR1 through regulation of inflammation.

Most significant, in addition to the reparative process, a faster healing time for hard and soft tissue may be able to reestablish the homeostasis of the alveolar ridge and limit the buccal bone remodeling. The mechanism by which MaR1 promotes socket bone fill is not yet fully understood. One possible pathway that was observed in our study is that the faster extraction wound closure may provide a protective effect for underlying socket bone fill. It is still unknown whether MaR1 has a direct action on osteoblasts or if it promotes socket bone fill indirectly through resolving inflammation or both. The extraction socket bone fill and ridge-remodeling process is a complex and coordinated event that includes coupling of osteoblast and osteoclasts in the context of bacterial challenge and inflammation. It has been shown that MaR1 can enhance phagocytosis and killing of oral pathogens (Wang et al. 2015) as well as counterregulate TNF- α (Gong et al. 2014), which has been shown to inhibit osteoblast differentiation (Gilbert et al. 2000). Taken together, this could be a potential indirect mechanism to facilitate socket wound healing and bone fill. In terms of

clinical implications, faster socket bone fill may shorten the edentulous ridge healing time before dental implant placement, or it may be beneficial for immediate implant placement cases to promote more rapid osseointegration. Preserved alveolar bone architecture is critical for an ideal implant placement.

Our study results demonstrated that there may be a therapeutic concentration window of MaR1. MaR1 is an endogenous mediator and is present in human tissue fluid, such as tears, milk, synovial fluid, and serum (Dalli and Serhan 2012; Giera et al. 2012; Colas et al. 2014; Arnardottir et al. 2016; English et al. 2017). These lipid mediators have their specific receptors with a lower bioactive range (typically at nano- to picomolar concentrations) as compared with other protein molecules (Serhan 2014). Based on the results of this study, the maximal effective dosage of MaR1 may be $\sim 0.05 \mu\text{g}/\mu\text{L}$ (equates to 131 nM), which is 10- to 100-times higher concentration as compared with most in vitro studies demonstrating a peak efficacy of 1 to 10 nM. Resolvin E1, another family of specialized proresolving lipid mediator, was used topically to treat experimental periodontitis, with similar concentrations of 0.5, 0.25, and 0.1 $\mu\text{g}/\mu\text{L}$. All concentrations showed similar

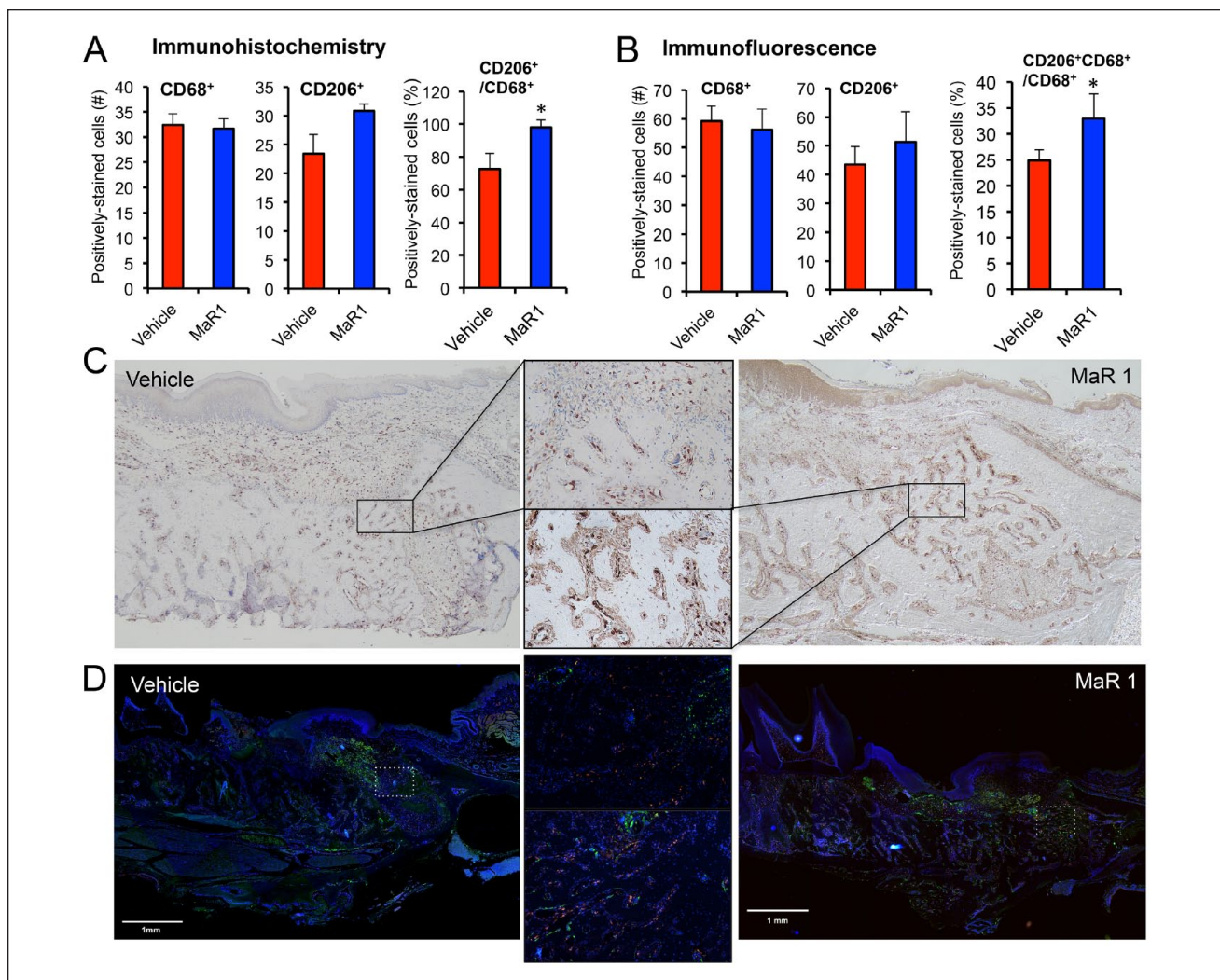


Figure 3. Maresin I (MaR1) regulates the relative expression ratio of M2-like macrophage surface marker CD206. Animals were sacrificed at day 10, and the en bloc section of the extraction socket was processed for histologic analysis and stained for CD68 and CD206 surface markers. Photos were taken at coronal, middle, and apical portions of the mesial root consistently, and quantifications of the positively stained cells were performed by a masked expert through immunohistochemistry and immunofluorescence. MaR1 (0.05 $\mu\text{g}/\mu\text{L}$) regulates (A) the relative ratio of CD206- to CD68-positive cells as well as (B) the relative ratio of double-positive cells. Results are presented as mean \pm SEM. $n = 4$, * $P < 0.05$ vs. vehicle. (C) Representative immunohistochemistry images of the stained CD206 marker in each group (4 \times). The area with higher magnification (20 \times) shows the coronal third of the socket. (D) Representative immunofluorescence merged images in each group (DAPI, blue; CD68, green; CD206, red). The area with higher magnification (20 \times) in the middle (vehicle group on the top) shows the coronal third of the socket. The scale bar represents 1-mm length.

results in limiting bone loss (Lee et al. 2016). The current study used a gelatin sponge carrier, which has been shown to be lipophilic (Kallinteri et al. 2001). The use of the gelatin sponge carrier with tissue glue was designed to assist in blood clot formation. The natural extraction healing without any carrier has been observed, and nearly 40% of the sockets achieved complete wound closure, which is consistent with the timeline in this study. The gelatin sponge and the tissue glue may have a limited effect on the extraction wound healing. Gelatin sponge as a carrier for MaR1 and its degradation, releasing, and pharmacokinetics should warrant further investigation.

Additionally, the MaR1 pathway stimulates macrophage phenotype switching from proinflammatory M1- to M2-like

macrophages in vitro and in vivo (Dalli et al. 2013; Marcon et al. 2013; Viola et al. 2016), and M2 phenotypes are responsible for healing and tissue regeneration (Martinez et al. 2009). Our study demonstrated that MaR1 increases CD206⁺ M2-like macrophages. An experimental periodontitis model showed that induction of M2 macrophages has protective effects on the alveolar bone (Zhuang et al. 2019). The mechanism of M2 macrophages and their specific roles in tooth extraction wound healing and tissue regeneration still require further study.

Finally, MaR1 ameliorated immediate postoperative pain scores, as observed with the 3 methods: grimace scale, tube chewing, and modified burrowing time. The pain score results showed significant differences only at postoperative day 1, and

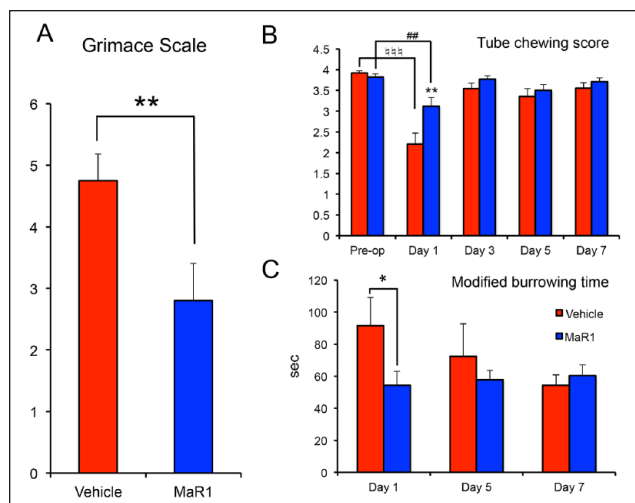


Figure 4. Maresin 1 reduces postoperative pain scores. One to 7 d after the tooth extraction, 3 pain scores and measurements were recorded and assessed for the postoperative discomfort. **(A)** Two 30-s video clips were randomly taken per cage after rat acclimation. Grimace scales were assessed by 2 calibrated masked examiners. $n = 8$ cages per group. **(B)** Standardized chewing tubes were given every 48 h and measured for destruction. A lower destruction score indicated a higher pain level. $n = 22$ tubes per group. **(C)** The time that rats spent in the plastic burrow tube were calculated. A greater time spent in the burrowing tube indicates a higher pain level. $n = 8$ cages per group. All the cages treated with MaR1 were grouped. Results are presented as mean \pm SEM. * $P < 0.05$ and ** $P < 0.01$ vs. vehicle control. ## $P < 0.01$ and ### $P < 0.001$ vs. preoperative in each group.

the scores returned to normal levels in both groups later on. This finding can be explained due to the fact that a simple extraction heals quite rapidly. MaR1 has been shown to reduce pain in different animal models (Gao et al. 2018; Zhang et al. 2018). The possible analgesic effects of MaR1 may have significant potential in clinical implications to reduce the postoperative pain and discomfort in patients.

The effect of MaR1 on delayed or compromised healing models may be more significant, such as aphthous ulcers or surgical trauma. Delivery of MaR1 has been demonstrated to aid in diabetic wound healing, as the local biosynthesis of MaR1 is compromised by the diabetic condition (Tang et al. 2013). The biosynthesis of MaR1 and its active metabolome in humans has been investigated and established (Dalli et al. 2013; Deng et al. 2014; Wang et al. 2015; Colas et al. 2016). Therefore, it will be of great interest to study the local biosynthesis and metabolome of MaR1 in the natural course of wound healing to further understand the best timing and dosage to optimize the delivery system for MaR1.

Conclusion

Within the limitation of this preclinical rat animal study for extraction socket healing, MaR1 reduced immediate postoperative pain scores, accelerated complete wound closure, stimulated more rapid socket bone fill, and preserved the alveolar ridge. MaR1 holds significant potential to promote oral

extraction wound healing and ridge preservation for dental implant reconstruction.



Author Contributions

C.W. Wang, contributed to conception, design, data acquisition, analysis, and interpretation, drafted and critically revised the manuscript; S.H. Yu, contributed to design, data acquisition, analysis, and interpretation, drafted and critically revised the manuscript; T. Fretwurst, L. Larsson, contributed to data acquisition and analysis, critically revised the manuscript; J.V. Sugai, Q. Jin, contributed to design and data acquisition, critically revised the manuscript; J. Oh, K. Lehner, contributed to data acquisition, critically revised the manuscript; W.V. Giannobile, contributed to conception, design, and data interpretation, critically revised the manuscript. All authors gave final approval and agree to be accountable for all aspects of the work.

Acknowledgments

The authors thank Dr. Laurie McCauley for her critical review of this manuscript and James Henderson for statistical consultation at the Center for Statistical Consultation and Research. We also thank Dr. Yao Yao for the technical support. This study was supported by the Michigan Institute for Clinical and Health Research from the University of Michigan (National Institutes of Health, ULRR024986) and the Department of Periodontics and Oral Medicine, School of Dentistry, University of Michigan. The authors declare no potential conflicts of interest with respect to the authorship and/or publication of this article.

ORCID iDs

C.W. Wang  <https://orcid.org/0000-0001-9679-4121>
W.V. Giannobile  <https://orcid.org/0000-0002-7102-9746>

References

- Abdulnour R-EE, Dalli J, Colby JK, Krishnamoorthy N, Timmons JY, Tan SH, Colas RA, Petasis NA, Serhan CN, Levy BD. 2014. Maresin 1 biosynthesis during platelet-neutrophil interactions is organ-protective. *Proc Natl Acad Sci U S A.* 111(46):16526–16531.
- Aguirre JI, Altman MK, Vanegas SM, Franz SE, Bassit AC, Wronski TJ. 2010. Effects of alendronate on bone healing after tooth extraction in rats. *Oral Dis.* 16(7):674–685.
- Akagi D, Chen M, Toy R, Chatterjee A, Conte MS. 2015. Systemic delivery of proresolving lipid mediators resolvin D2 and maresin 1 attenuates intimal hyperplasia in mice. *FASEB J.* 29(6):2504–2513.
- Amler MH, Johnson PL, Salman I. 1960. Histological and histochemical investigation of human alveolar socket healing in undisturbed extraction wounds. *J Am Dent Assoc.* 61:32–44.
- Araujo MG, Lindhe J. 2005. Dimensional ridge alterations following tooth extraction: an experimental study in the dog. *J Clin Periodontol.* 32(2):212–218.
- Arnardottir H, Orr SK, Dalli J, Serhan CN. 2016. Human milk proresolving mediators stimulate resolution of acute inflammation. *Mucosal Immunol.* 9(3):757–766.
- Avila-Ortiz G, Elangovan S, Kramer K, Blanchette D, Dawson D. 2014. Effect of alveolar ridge preservation after tooth extraction. *J Dent Res.* 93(10):950–958.
- Bassir S, Alhareky M, Wangsrimongkol B, Jia Y, Karimbux N. 2018. Systematic review and meta-analysis of hard tissue outcomes of alveolar ridge preservation. *Int J Oral Maxillofac Implants.* 33(5):979–994.
- Bui CH, Seldin EB, Dodson TB. 2003. Types, frequencies, and risk factors for complications after third molar extraction. *J Oral Maxillofac Surg.* 61(12):1379–1389.

- Cezar TLC, Martinez RM, Rocha CD, Melo CPB, Vale DL, Borghi SM, Fattori V, Vignoli JA, Camilios-Neto D, Baracat MM, et al. 2019. Treatment with maresin 1, a docosahexaenoic acid-derived pro-resolution lipid, protects skin from inflammation and oxidative stress caused by UVB irradiation. *Sci Rep.* 9(1):3062.
- Colas RA, Shinohara M, Dalli J, Chiang N, Serhan CN. 2014. Identification and signature profiles for pro-resolving and inflammatory lipid mediators in human tissue. *Am J Physiol Cell Physiol.* 307(1):C39–C54.
- Colas RA, Dalli J, Chiang N, Vlasakov I, Sanger JM, Riley IR, Serhan CN. 2016. Identification and actions of the maresin 1 metabolome in infectious inflammation. *J Immunol.* 197(11):4444–4452.
- Dalli J, Serhan CN. 2012. Specific lipid mediator signatures of human phagocytes: microparticles stimulate macrophage efferocytosis and pro-resolving mediators. *Blood.* 120(15):e60–e72.
- Dalli J, Zhu M, Vlasenko NA, Deng B, Haeggstrom JZ, Petasis NA, Serhan CN. 2013. The novel 13S,14S-epoxy maresin is converted by human macrophages to maresin1 (MaR1), inhibits leukotriene A4 hydrolase (LTA4H), and shifts macrophage phenotype. *FASEB J.* 27(7):2573–2583.
- Das A, Sinha M, Datta S, Abas M, Chaffee S, Sen CK, Roy S. 2015. Monocyte and macrophage plasticity in tissue repair and regeneration. *Am J Pathol.* 185(10):2596–2606.
- Deng B, Wang CW, Arnardottir HH, Li Y, Cheng CY, Dalli J, Serhan CN. 2014. Maresin biosynthesis and identification of maresin 2, a new anti-inflammatory and pro-resolving mediator from human macrophages. *PLoS One.* 9:e102362.
- English JT, Norris PC, Hodges RR, Dartt DA, Serhan CN. 2017. Identification and profiling of specialized pro-resolving mediators in human tears by lipid mediator metabolomics. *Prostaglandins Leukot Essent Fatty Acids.* 117:17–27.
- Gao J, Tang C, Tai LW, Ouyang Y, Li N, Hu Z, Chen X. 2018. Pro-resolving mediator maresin 1 ameliorates pain hypersensitivity in a rat spinal nerve ligation model of neuropathic pain. *J Pain Res.* 11:1511–1519.
- Garlet GP, Giannobile WV. 2018. Macrophages: the bridge between inflammation resolution and tissue repair? *J Dent Res.* 97(10):1079–1081.
- Giera M, Ioan-Facsinay A, Toes R, Gao F, Dalli J, Deelder AM, Serhan CN, Mayboroda OA. 2012. Lipid and lipid mediator profiling of human synovial fluid in rheumatoid arthritis patients by means of LC-MS/MS. *Biochim Biophys Acta.* 1821(11):1415–1424.
- Gilbert L, He X, Farmer P, Boden S, Kozlowski M, Rubin J, Nanes MS. 2000. Inhibition of osteoblast differentiation by tumor necrosis factor- α . *Endocrinology.* 141(11):3956–3964.
- Gong J, Wu ZY, Qi H, Chen L, Li HB, Li B, Yao CY, Wang YX, Wu J, Yuan SY, et al. 2014. Maresin 1 mitigates LPS-induced acute lung injury in mice. *Br J Pharmacol.* 171(14):3539–3550.
- Jin Q, Anusaksathien O, Webb SA, Printz MA, Giannobile WV. 2004. Engineering of tooth-supporting structures by delivery of PDGF gene therapy vectors. *Mol Ther.* 9(4):519–526.
- Kallinteri P, Antimisiaris SG. 2001. Solubility of drugs in the presence of gelatin: effect of drug lipophilicity and degree of ionization. *Int J Pharm.* 221(1–2):219–226.
- Krishnamoorthy N, Burkett PR, Dalli J, Abdulnour R-EE, Colas R, Ramon S, Phipps RP, Petasis NA, Kuchroo VK, Serhan CN, et al. 2015. Cutting edge: maresin-1 engages regulatory T cells to limit type 2 innate lymphoid cell activation and promote resolution of lung inflammation. *J Immunol.* 194(3):863–867.
- Kuroshima S, Kovacic BL, Kozloff KM, McCauley LK, Yamashita J. 2013. Intra-oral PTH administration promotes tooth extraction socket healing. *J Dent Res.* 92(6):553–559.
- Lee CT, Teles R, Kantarci A, Chen T, McCafferty J, Starr JR, Brito LC, Paster BJ, Van Dyke TE. 2016. Resolvin E1 reverses experimental periodontitis and dysbiosis. *J Immunol.* 197(7):2796–2806.
- Lin Z, Rios HF, Volk SL, Sugai JV, Jin Q, Giannobile WV. 2011. Gene expression dynamics during bone healing and osseointegration. *J Periodontol.* 82(7):1007–1017.
- Martinez FO, Helming L, Gordon S. 2009. Alternative activation of macrophages: an immunologic functional perspective. *Annu Rev Immunol.* 27:451–483.
- Marcon R, Bento AF, Dutra RC, Bicca MA, Leite DF, Calixto JB. 2013. Maresin 1, a proresolving lipid mediator derived from omega-3 polyunsaturated fatty acids, exerts protective actions in murine models of colitis. *J Immunol.* 191(8):4288–4298.
- Oliver V, De Rantere D, Ritchie R, Chisholm J, Hecker KG, Pang DS. 2014. Psychometric assessment of the rat grimace scale and development of an analgesic intervention score. *PLoS One.* 9(5):e97882.
- Pagni G, Pellegrini G, Giannobile WV, Rasperini G. 2012. Postextraction alveolar ridge preservation: biological basis and treatments. *Int J Dent.* 2012:151030.
- Schropp L, Kostopoulos L, Wenzel A. 2003. Bone healing following immediate versus delayed placement of titanium implants into extraction sockets: a prospective clinical study. *Int J Oral Maxillofac Implants.* 18(2):189–199.
- Serhan CN. 2014. Pro-resolving lipid mediators are leads for resolution physiology. *Nature.* 510(7503):92–101.
- Serhan CN, Dalli J, Karamnov S, Choi A, Park CK, Xu ZZ, Ji RR, Zhu M, Petasis NA. 2012. Macrophage proresolving mediator maresin 1 stimulates tissue regeneration and controls pain. *FASEB J.* 26(4):1755–1765.
- Serhan CN, Yang R, Martinod K, Kasuga K, Pillai PS, Porter TF, Oh SF, Spite M. 2009. Maresins: novel macrophage mediators with potent anti-inflammatory and pro-resolving actions. *J Exp Med.* 206(1):15–23.
- Sotocinal SG, Sorge RE, Zaloum A, Tuttle AH, Martin LJ, Wieskopf JS, Mapplebeck JC, Wei P, Zhan S, Zhang S, et al. 2011. The rat grimace scale: a partially automated method for quantifying pain in the laboratory rat via facial expressions. *Mol Pain.* 7:55.
- Tang Y, Zhang MJ, Hellmann J, Kosuri M, Bhatnagar A, Spite M. 2013. Proresolution therapy for the treatment of delayed healing of diabetic wounds. *Diabetes.* 62(2):618–627.
- Vieira AE, Repeke CE, Ferreira Junior S de B, Colavite PM, Bigueti CC, Oliveira RC, Assis GF, Taga R, Trombone AP, Garlet GP. 2015. Intramembranous bone healing process subsequent to tooth extraction in mice: micro-computed tomography, histomorphometric and molecular characterization. *PLoS One.* 10(5):e0128021.
- Viniegra A, Goldberg H, Çil Ç, Fine N, Sheikh Z, Galli M, Freire M, Wang Y, Van Dyke TE, Glogauer M, et al. 2018. Resolving macrophages counter osteolysis by anabolic actions on bone cells. *J Dent Res.* 97(10):1160–1169.
- Viola JR, Lemnitzer P, Jansen Y, Csaba G, Winter C, Neideck C, Silvestre-Roig C, Dittmar G, Döring Y, Drechsler M, et al. 2016. Resolving lipid mediators maresin 1 and resolvin D2 prevent atheroprotection in mice. *Circ Res.* 119(9):1030–1038.
- Wang CW, Colas RA, Dalli J, Arnardottir HH, Nguyen D, Hasturk H, Chiang N, Van Dyke TE, Serhan CN. 2015. Maresin 1 biosynthesis and proresolving anti-infective functions with human-localized aggressive periodontitis leukocytes. *Infect Immun.* 84(3):658–665.
- Wodarski R, Delaney A, Ultenius C, Morland R, Andrews N, Baastrup C, Bryden LA, Caspani O, Christoph T, Gardiner NJ, et al. 2016. Cross-centre replication of suppressed burrowing behaviour as an ethologically relevant pain outcome measure in the rat: a prospective multicentre study. *Pain.* 157(10):2350–2365.
- Zhang L, Terrando N, Xu ZZ, Bang S, Jordt SE, Maixner W, Serhan CN, Ji RR. 2018. Distinct analgesic actions of DHA and DHA-derived specialized pro-resolving mediators on post-operative pain after bone fracture in mice. *Front Pharmacol.* 9:412.
- Zhuang Z, Yoshizawa-Smith S, Glowacki A, Maltos K, Pacheco C, Shehabeldin M, Mulkeen M, Myers N, Chong R, Verdelsis K, et al. 2019. Induction of M2 macrophages prevents bone loss in murine periodontitis models. *J Dent Res.* 98(2):200–208.